NACA RM L53F16

NACA

RESEARCH MEMORANDUM

SOME INFORMATION ON THE STRENGTH OF THICK-SKIN WINGS WITH MULTIWEB AND MULTIPOST STABILIZATION

By Roger A. Anderson, Richard A. Pride,
and Aldie E. Johnson, Jr.

Langley Aeronautical Laboratory
Langley Field, Va.

NATIONAL ADVISORY COMMITTEE
FOR AERONAUTICS

WASHINGTON
August 27, 1953

NACA RM L53F16

NATIONAL ADVISORY COMMITTEE FOR AERONAUTICS

RESEARCH MEMORANDUM

SOME INFORMATION ON THE STRENGTH OF THICK-SKIN WINGS WITH MULTIWEB AND MULTIPOST STABILIZATION

By Roger A. Anderson, Richard A. Pride,
and Aldie E. Johnson, Jr.

SUMMARY

The preliminary results of strength tests on thick-skin wing structures are described. Some of the factors which have a major influence on the buckling behavior and strength of multiweb and multipost stiffened construction are illustrated by the data presented, and the conditions under which a combination of multiweb and multipost construction may be used are discussed. Also given are the results of bending tests on hollow circular-arc airfoils.

INTRODUCTION

A current investigation by the Langley Structures Research Division is concerned with obtaining experimental data on the strength characteristics of thin wings with thick cover skins under various loadings. The beam structures tested to date have incorporated the essential structural features of multiweb and multipost stiffened wing construction. A small number of hollow circular-arc airfoil specimens have also been tested to failure in pure bending.

This paper describes the preliminary results of these programs and points out some of the factors which influence the buckling behavior and strength characteristics of the various constructions.

SYMBOLS

Symbols for dimensions of test specimens are shown in figure 2. In addition, the following definitions are given for symbols used in the paper.

I moment of inertia of specimen cross sections, $in.^4$

M_B bending moment at buckling, in-kips

M_f bending moment at failure, in-kips

T_B torque moment at buckling, in-kips

T_f torque moment at failure, in-kips

σ_f average stress in cover skins at failure, $\frac{M_f H}{2I}$, ksi

F_1 distance between back of channel web and center line of rivets, in.

F_2 width of web attachment flange, in.

TEST SPECIMENS

Figure 1 shows the general types of wing constructions which are considered in this paper. The first cross section illustrated is a circular-arc airfoil without internal stiffening. The strength of such an airfoil when subjected to a bending moment serves as a convenient lower limit to which the strength of internally stiffened thick-skin airfoils may be compared. The second wing structure shown is the familiar multiweb beam. The role played by full-depth webs in the stabilization of cover skins will be discussed in the light of recent tests and theory. A variation of the multiweb beam is the multipost stiffened beam, in which a line of posts and stiffeners is used to replace a solid web for production reasons or for weight economy.

A master drawing of each of the three types of test specimens used to obtain strength data on these wing constructions is shown in figure 2. Numerical values of the nominal specimen dimensions are listed in tables I, II, and III. Also listed in the tables are the buckling and failure moments for the specimens. As noted in the tables, the circular-arc airfoils and the multiweb beams were constructed of 75S-T6 aluminum alloy and the multipost stiffened beams were constructed of 14S-T6 aluminum tubing with 75S-T6 aluminum stiffening.

All beam specimens were tested in the combined load testing machine of the Langley structures research laboratory. Bending and torque moments at buckling and failure were measured with an accuracy of ± 1 percent.

PRESENTATION OF RESULTS

Circular-Arc Airfoils

The strength of long circular-arc airfoils in pure bending is shown in figure 3. Here the strength is defined in terms of the bending stress developed in the middle plane of the cover skin at the midchord of the airfoil at failure. This stress is plotted as a function of the ratio of beam thickness to skin thickness H/t_S for various values of H/c, the thickness ratio for the cross section. The curves for a 4-, an 8-, and a 10-percent-thick airfoil are derived from an ultimate-strength theory given in reference 1. The theory is for an infinitely long beam and is based upon the progressive flattening of the cross section as the beam bends, the so-called "Brazier effect," and leads to the following ultimate stress formula:

$$\sigma_f = 1.14E\left(\frac{H}{c}\right)^2 \frac{t_S}{H}$$

The circles are experimental results obtained on beams of plan-form aspect ratio 3 between rib stations (see table I) and they are in fair agreement with equation (1).

It is seen that, because of the cross-sectional flattening that occurs during bending of a hollow beam, the stress level at failure is generally low. The structural strength problem for thick-skin airfoils thus resolves into providing a system of internal supports which will prevent cross-sectional distortion and enable the thick skin to carry the required flight loads.

Multiweb Beams

One practical type of internal structure consists of full-depth spanwise webs. The stabilization provided the wing cover skins by internal spanwise webs is principally dependent upon the depthwise stiffness of the webs. It is desirable that the required depthwise stiffness be achieved without structural complexity and at the least possible weight.

Beams with formed webs.- A commonly used type of web consists of a channel formed from sheet material. The results of pure bending tests on multiweb beams in which the spacing and depth of formed-channel webs have been varied are shown in figure 4. The test specimens consisted of three-cell beams of constant depth and of sufficient length to allow the free formation of a buckle pattern (see fig. 2 and table II). The

channel-type webs were cold formed from sheet material to a $4t_w$ bend radius between the web and the attachment flanges. The ratio of web thickness to cover skin thickness is 0.41. The line of rivets attaching the webs to the cover skins was kept as close to the plane of the web as permitted by the corner radius. The diameter and pitch of the rivets was such that the potential strength of the structure (see ref. 2) should have been developed. No rivet failures were encountered in the tests.

The average stress in the cover skins at failure has been defined as $\sigma_f = \frac{M_f H}{2I}$ and is plotted against the H/t_s ratio for the beams (see fig. 4). The various beams were designed to provide a ratio of cell width to skin thickness b_s/t_s of 25, 30, 40, and 60. For each value of b_s/t_s, beams were tested in which the depth of the webs was varied to cover a range of ratios of beam thickness to skin thickness. Curves have been faired through the test data obtained.

Although the stress level at failure increases as b_s/t_s is decreased, it was noted that for the beams with b_s/t_s equal to 25 and 30 the failure stresses were lower than the local buckling stresses that would be predicted for beams with integral webs (ref. 3). As will be pointed out later, these low failure stresses are a result of the skin-web joint flexibility of beams with formed-channel webs. Also, as H/t_s increases, the stress level at failure tends to decrease because of the loss of stiffness in the webs due to local buckling under the beam bending stresses.

Figure 5 presents the effect of changes in web-skin thickness ratio on the $\sigma_f = \frac{M_f H}{2I}$ stress at failure for the multiweb beams tested in this investigation. The data are obtained from beams with a ratio of b_s/t_s equal to 30. Since the riveting of the beams was changed as t_w/t_s was changed (see table II), the variation in strength shown in figure 5 may not be necessarily attributed solely to the changes in t_w/t_s. The effect of increasing the web thickness relative to the cover thickness is to increase substantially the stress level at failure.

Beams with extruded webs or cap members.- Extruded angles are often used to make the attachment of webs to cover skins and experimental evidence indicates that the integral plate-buckling theory of references 3 and 4 may be used to predict the beam buckling stress. The relationship between the buckling stress and the failing stress, however, has not been established for a range of beam proportions. For a given b_s/t_s value, the post-buckling strength may be presumed to be dependent upon the web proportions as well as upon the rivet strength. Such a dependency has

previously been found for the local crippling strength of short stiffened compression panels (refs. 2, 5, and 6).

Until sufficient experimental data have been accumulated on the failing stresses in bending of multiweb beams with extruded webs (or cap members) it would appear that the available data on the failing stresses of short compression panels with extruded stiffeners would be useful in making strength predictions for multiweb beams in bending. For example, extensive data exist in references 5 and 6 on the local crippling strength of strongly riveted, short 75S-T6 aluminum-alloy compression panels with extruded Z-stiffeners. The local crippling failures observed in these short panels are very similar to the compression surface failures that are encountered in multiweb-beam tests. It, therefore, seems reasonable that the panel-failure data may be applied to make strength predictions for geometrically similar multiweb beams, that is, beams with webs of the same cross-sectional details in the region of attachment to skin as the extruded Z-stiffeners (minus their outstanding flanges). Such a strength prediction for multiweb beams with a ratio of web thickness to skin thickness of 0.41 is presented in figure 6.

In the preparation of figure 6, it was assumed that, for given values of b_s/t_s and t_w/t_s, a multiweb beam which will buckle at the same stress as a Z-stiffened panel will also develop an average cover skin stress at failure equal to the average stress in the panel at failure. With this assumption, the web depth of the equivalent strength multiweb beams was determined from a comparison of the buckling-stress charts presented in references 3 and 7. This comparison indicated that, for given values of b_s/t_s and t_w/t_s, multiweb beams in bending with a web depth of $2\frac{1}{2}$ times the compression-panel Z-stiffener depth will buckle at the same value of skin compressive stress.

The trend of the curves presented in figure 6 is very similar to the trend of experimental data given in figure 4. A comparison of these two figures, however, indicates that with 75S-T6 aluminum alloy a failing stress increase ranging from 25 to 35 percent is obtained by a change from formed sheet-metal webs (with a $4t_w$ bend radius between web and attachment flange) to a square-cornered extrusion connecting the webs and covers. This strength increase is attributed to the improved support stiffness of webs with square corners which permit rivets to be driven closer to the web plane, thus reducing attachment flange flexibility.

Bend-radius investigation.- Since it was apparent that the support stiffness of webs could be strongly influenced by the detail design of the attachment flange region, four beams were built and tested specifically to explore the effect of design changes in this region. The only variations in the otherwise nominally alike beams were changes in the bend radius between the webs and their attachment flanges. These changes

are shown in figure 7. The first beam had square-cornered webs (with small fillets) which are achievable with an extrusion, and the other beams cover a range of bend radii encountered in production practice with sheet material. In each case the joint was strongly riveted and the eccentricity was minimized by keeping the line of rivets as close to the plane of the webs as the corner radii permitted. Details of the riveting are given in table II.

The results of pure bending tests on these beams are shown in the bar graph (fig. 7), and the variation in the stress at failure is seen to be very substantial. Compared with the $4t_w$ radius specimen, which is representative of best production practice with 75S-T6 sheet material, the specimen with the square-cornered extrusion carried a 40 percent greater bending moment. It is estimated that a further increase of a few percent in beam strength would be obtained if the joint stiffness were further improved, for example, by the use of an extruded T-connection between webs and covers. The strength increase obtained in these four tests by decreasing the radius between the webs and their attachment flanges is of the order of magnitude of the strength increase predicted from extruded-Z-stiffened-panel data as explained in the previous section.

The tests also afforded an opportunity to study the change in buckling mode of the specimens as the effective depthwise stiffness of the webs was changed. In the beams with the formed-channel webs, skin buckling occurred with "washboard" buckles; that is, buckles with only transverse nodes indicating that deflections of the web attachment flanges as well as the cover skin were occurring. In the beam with the square-cornered webs, local buckling of the cover skin and webs occurred with longitudinal nodes along the web attachment lines.

The buckling theory presented in reference 8 takes into account the depthwise stiffness of eccentrically attached webs, and the correlation of this theory with a series of multiweb beam tests is shown in figure 8. The solid-line curve in figure 8 gives the buckling-stress prediction for the test beams built with a $4t_w$ bend radius in the formed-channel webs and the symbols indicate the experimentally observed buckling stresses for the test beams. The dashed-line curve is the buckling-stress prediction for these same beams using the integral web theory of reference 3. The substantial reduction in the buckling stress due to the depthwise flexibility of formed-channel webs accounts for the relatively low failure stresses of these beams, which are plotted in figure 4.

Combined bending and torsion of multiweb beams.- Preliminary tests have been made in which multiweb beams were subjected to combined bending and torsion and pure-torsion loads. These tests were made to determine possible procedures for predicting the interaction of combined stresses on the failing strengths of this type of structure.

Under a pure-torsion load it is proposed that plane diagonal-tension theory (ref. 9) can be used to calculate the ultimate shear strength of the cover skins by assuming that the webs act as uprights. For a three-cell beam tested in pure torsion, this procedure gave a strength prediction that was about 15 percent conservative. The beam had closing webs that were as thick as the cover skins in order to carry the shear flow around the box and the failure was confined to a forced crippling of the two lighter interior webs. Although this agreement was considered satisfactory, better agreement might be expected for test beams with a greater number of interior webs.

The combined-load tests indicated that the assumption of a parabolic-type interaction between torsional and bending moments leads to a slightly conservative strength prediction. At the present time, therefore, it appears that for multiweb beams with formed-channel webs, diagonal-tension theory may be used to estimate the strength under a pure-torsional moment and data such as that presented in figure 4 may be used to predict the strength under a pure-bending moment. For combinations of these two loadings, a parabolic interaction may be assumed.

Multipost Stiffened Beams

The multipost stiffened wing structure may be characterized as essentially a multiweb structure in which a number of the full-depth webs have been replaced by lines of small stiffeners connected by spaced vertical posts or uprights, as shown in figure 1. The desirability of such a replacement for production reasons has been discussed in reference 10. A viewpoint expressed in reference 11 was that, for a certain intermediate range of wing depths, a combination of stiffeners and posts may provide a more efficient means of stabilizing the covers than either stiffeners of large moment of inertia or full-depth webs. In this depth range, the solid webs of a multiweb beam are subject to considerable buckling unless they are stiffened by uprights or increased in thickness, either of which alternatives lead to the webs becoming a considerable portion of the total beam weight. Theoretical studies have indicated that for equal or less weight than a solid web, a combination of posts and stiffeners of small moment of inertia can perform some of the functions of a web, depending upon the loading conditions.

Multipost stiffened beams in pure bending.- The theoretical calculations reported in reference 11 showed that in pure bending a combination of posts and small stiffeners can constrain the compression cover to buckle in a desirable manner, that is, it can force a longitudinal node to form along the line of stiffeners and posts. The combinations of stiffener stiffness, post stiffness, post spacing, and so forth required to form a node were established and this behavior has been confirmed by tests reported in reference 10 as well as tests described in this paper.

The present test beams were constructed from rectangular cross-section tubes of 14S-T6 aluminum alloy. The purpose of these tests was to observe the buckling behavior and compare the strength of the beams when stiffened along the longitudinal center line by several different post stiffener combinations as well as by a solid web. For the beams stiffened by the post stiffener combinations, the posts were riveted to the stiffeners with a single rivet at each end, simulating a pin-ended condition. The solid web was a channel formed to a 4t bend radius. The weight of the center line supports in each of these beams was the same. In a control test, the unstiffened tube was also buckled and failed. A description of these test specimens is given in table III and figure 2.

The results of the comparative tests are given in figure 9. As shown by the shaded portions of the bar graphs, the solid web and each of the post stiffener combinations raised the buckling stress of the tube from about 6,000 psi, when unstiffened, to about 23,000 psi. In these four tests, local buckling of the skin occurred with a longitudinal node along the center-line support. Just prior to failure, however, the longitudinal node along the support disappeared with resulting deflection of the support. Failure occurred as a consequence of the large forces on the supports associated with the deflection. On the basis of these few tests, it appears that small, rather than large, post spacings are slightly more effective in resisting final failure and that for equal weight a combination of stiffeners and posts can be as effective as a solid formed web in stabilizing the compression cover in a pure-bending test.

Multipost stiffened beams in combined bending and torsion.- When torsion is combined with bending, the role played by the posts in stabilizing the beam depends upon a number of factors in addition to their axial stiffness and spacing. The most important of these factors are the ratio of shear stress to bending stress present in the beam covers and the end fixity and bending stiffness of the posts. A few tests have been made to evaluate the relative importance of these factors.

The test specimens used for the combined-load tests were similar in construction to those used in the bending tests (see table III) with the exception of the attachment between post and stiffener. The posts were connected in a manner which introduced an undetermined amount of end restraint to the posts with the exception of one specimen which had a pin connection between posts and stiffeners (as in the bending specimens). All specimens were built with the same stiffener and post cross sections and the ratio of post spacing to cell width was unity. The results of combined-loading tests on these specimens is shown in figure 10 where the shear stress in the cover skin arising from torsion is plotted against the compressive stress arising from bending.

The solid interaction curves were faired through the circle symbols which represent tests on specimens having posts with end restraint. Thus, in these tests the stiffeners and posts were capable of developing some Vierendeel truss action to resist cover buckling. The buckling stresses for the two tests with pin-ended posts are shown by the square symbols on the shear and compressive stress axes. In pure bending, the results with pinned and restrained posts are in agreement as would be expected since the line of posts and stiffeners are capable of forming a longitudinal node at buckling and Vierendeel truss action does not come into play. The small spread between the buckling-stress results with pinned and restrained posts in pure torsion, however, is attributed to Vierendeel truss action. Diagonal shear buckling occurred in each of these tests with the buckle nodes passing through the post locations on the stiffeners. With this type of buckling, Vierendeel truss action causes an increase in the effective stiffener stiffness. However, as can be seen from the buckling charts of reference 12, large increases in stiffener stiffness produce only relatively small changes in the buckling stress of longitudinally stiffened plates stressed in shear.

The shape of the experimentally determined buckling interaction curve is very favorable in that a high percentage of the buckling loads in pure torsion and pure bending alone must be applied in combination to cause buckling. Along the portion of the interaction curve associated with high ratios of bending stress to shear stress the post-stiffener combination provides about the same stability to the compression cover as would be expected for a solid web.

Interaction curves for these beams were also computed with the simplifying assumption that the side walls of the tube provided simple support for the covers. The results of a computation for the buckling stress combinations for the covers stiffened by the longitudinal stiffeners alone are shown by the short dashed-line curve (fig. 10). With the addition of closely spaced, infinitely stiff posts, pin connected to the stiffeners, theory indicates that buckling should occur at the stress combinations given by the dashed-line curve. It is noticed that in pure shear the post-stiffener combination is theoretically no more effective than the stiffeners alone, but, as the ratio of bending to shear stress increases, the posts provide a stabilizing effect on the covers.

The spread between the dashed-line curve and the solid-line buckling-interaction curve established by tests is attributed to the edge restraints offered by the side walls of the tube during buckling. These edge restraints are especially large during the formation of a continuous skewed buckle around the unequal width walls of a rectangular tube buckling in shear. At the other loading extreme, pure bending, these continuity restraints are not as large and the tests are in better agreement with the simplified theory.

CONCLUDING REMARKS

The preliminary results of the tests on thick-skin wing structures described in this paper illustrate the fact that the effectiveness of internal supports for the skin is highly dependent on their depthwise stiffness characteristics. These stiffness characteristics in turn have been shown to be strongly influenced by fabrication details such as corner bend radii, eccentricity of rivet lines on attachment flanges, and strength of riveting. The effect of these items on beam strength is such that they assume the importance of major design parameters when high stress levels are to be developed in a built-up structure.

Although the desirability of replacing some of the webs in a multiweb structure by lines of small stiffeners and posts has been explored in relatively few tests, these tests have indicated that such a replacement can be made without a loss in structural efficiency under certain loading conditions. This replacement will improve interior accessibility and for a certain range of wing depth may reduce the weight of the internal structure.

Langley Aeronautical Laboratory,
National Advisory Committee for Aeronautics,
Langley Field, Va., May 27, 1953.

REFERENCES

1. Fralich, Robert W., Mayers, J., and Reissner, Eric: Behavior in Pure Bending of a Long Monocoque Beam of Circular-Arc Cross Section. NACA TN 2875, 1953.

2. Dow, Norris F., and Hickman, William A.: Effect of Variation in Rivet Diameter and Pitch on the Average Stress at Maximum Load for 24S-T3 and 75S-T6 Aluminum-Alloy Flat, Z-Stiffened Panels that Fail by Local Instability. NACA TN 2139, 1950.

3. Schuette, Evan H., and McCulloch, James C.: Charts for the Minimum-Weight Design of Multiweb Wings in Bending. NACA TN 1323, 1947.

4. Eggwertz, Sigge F.: Buckling Stresses of Box-Beams Under Pure Bending. Rep. No. 33; Aero. Res. Inst. of Sweden (Stockholm), 1950.

5. Hickman, William A., and Dow, Norris F.: Data on the Compressive Strength of 75S-T6 Aluminum-Alloy Flat Panels With Longitudinal Extruded Z-Section Stiffeners. NACA TN 1829, 1949.

6. Hickman, William A., and Dow, Norris F.: Data on the Compressive Strength of 75S-T6 Aluminum-Alloy Flat Panels Having Small, Thin, Widely Spaced, Longitudinal Extruded Z-Section Stiffeners. NACA TN 1978, 1949.

7. Gallaher, George L., and Boughan, Rolla B.: A Method of Calculating the Compressive Strength of Z-Stiffened Panels That Develop Local Instability. NACA TN 1482, 1947.

8. Anderson, Roger A., and Semonian, Joseph W.: Charts Relating the Compressive Buckling Stress of Longitudinally Supported Plates to the Effective Deflectional and Rotational Stiffness of the Supports. NACA TN 2987, 1953.

9. Kuhn, Paul, Peterson, James P., and Levin, L. Ross: A Summary of Diagonal Tension. Part I - Methods of Analysis. NACA TN 2661, 1952.

10. Badger, D. M.: Notes on the Analysis and Design of Multi-Post Stiffened Wings. Preprint No. 393, S.M.F. Pub. Fund Preprint, Inst. Aero. Sci., Jan. 1953.

11. Anderson, Roger A., Wilder, Thomas W., III, and Johnson, Aldie E., Jr.: Preliminary Results of Stability Calculations for the Bending of Box Beams with Longitudinally Stiffened Covers Connected by Posts. NACA RM L52K10a, 1952.

12. Crate, Harold, and Lo, Hsu: Effect of Longitudinal Stiffeners on the Buckling Load of Long Flat Plates Under Shear. NACA TN 1589, 1948.

TABLE I

DIMENSIONS AND TEST DATA FOR CIRCULAR-ARC BEAMS

H/t_s	H/C	t_s, in.	C, in.	L, in. (a)	R, in.	M_f, in-kips
3.3	0.04	3/8	40	120	250	56.75
7.6	.08	3/8	40	120	125	242.8
10.5	.10	3/8	40	120	93.75	408.9

[a]Test length exclusive of end attachments.

NACA

TABLE II

DIMENSIONS AND TEST DATA FOR MULTIWEB BEAMS

H/t_s	b_s/t_s	t_w/t_s	t_s, in.	C, in.	L, in. (a)	F_1, in.	F_2, in.	r/t_w	Rivets		M_n, in-kips	M_f, in-kips
									Diam., in.	Pitch, in.		
13.6	25	0.41	0.125	10.37	20.62	0.48	0.76	4	5/16	9/16	90.5	104.5
17.7	↓	↓	↓	↓	20.62	↓	↓	↓	↓	↓	126.0	146.0
25.9					20.62						190.0	218.0
34.0					25.12						209.0	267.5
50.4					35.25						[b]234.0	394.0
13.6	30			12.26	23.44						109.0	119.0
17.7	↓			↓	23.44						128.0	139.0
25.9					23.44						179.0	204.5
34.0					25.12						240.0	269.0
50.4					35.25						[b]260.0	388.0
13.6	40			16.01	29.62						96.2	110.7
17.7	↓			↓	29.62						126.0	148.0
25.9					29.62						161.0	196.0
34.0					29.62						236.0	265.0
50.4					35.25						[b]312.0	385.0
13.6	60			23.51	42.00						65.0	124.0
17.7	↓			↓	↓						80.0	156.0
25.9											114.0	234.0
34.0											157.0	307.0
50.4											242.0	430.0
20.5	30	.63	.081	8.05	16.88	.41	.60		1/8	3/8	53.0	61.8
39.4		.63	.081	↓	19.88	.41	.60		1/8	3/8	112.0	116.3
77.2		.63	.081		35.25	.41	.60		1/8	3/8	[b]120.0	211.0
9.4		.26	.188	18.18	33.00	.53	.91		1/4	3/4	208.0	217.0
17.6			.188	↓	33.00	.53	.91		1/4	3/4	370.0	388.0
33.9			.188		35.25	.53	.91	↓	1/4	3/4	[b]604.0	715.0
21.7			.250	24.00	42.20	.47	.94	0	5/16	15/16	1,380	1,640
					41.30	.54	1.00	2			1,340	1,400
					39.80	.66	1.13	4			908.0	1,220
					39.80	.79	1.26	6			880.0	1,045

[a]Test length exclusive of end attachment.
[b]Denotes buckling initiated in webs.

NACA

TABLE III

DIMENSIONS AND TEST DATA FOR POST-STIFFENED BEAMS

H/t_s	l/b_s	t_s, in.	b_s, in.	L, in. (a)	Post	M_B, in-kips	M_f, in-kips	T_B, in-kips	T_f, in-kips
41	–	0.125	5.06	31.56	–	46.0	225	–	–
41	2	↓	↓	39.75	$\frac{1}{8} \times \frac{7}{8} \times \frac{7}{8}$ ∠	165	284	–	–
41	1	↓	↓	39.75	$\frac{1}{16} \times \frac{7}{8} \times \frac{7}{8}$ ∠	171	294	–	–
41	1/2	↓	↓	39.75	$\frac{1}{16} \times \frac{1}{2} \times \frac{3}{8}$ ∠	181	320	–	–
41	–	↓	↓	41.56	(b)	178	266	–	–
41	1	↓	↓	60.00	$\frac{1}{16} \times \frac{1}{2} \times \frac{1}{2}$ ∠	–	–	231	233
41	1	↓	↓	60.00	↓	160	255	140	140
41	1	↓	↓	60.00	↓	156	210	190	190
41	1	↓	↓	60.00	(c) ↓	–	–	210	231

[a] Test length exclusive of end attachments.
[b] Channel web with $t_w = 0.051$ formed to 4t bend radius.
[c] Pin-end post.

NACA

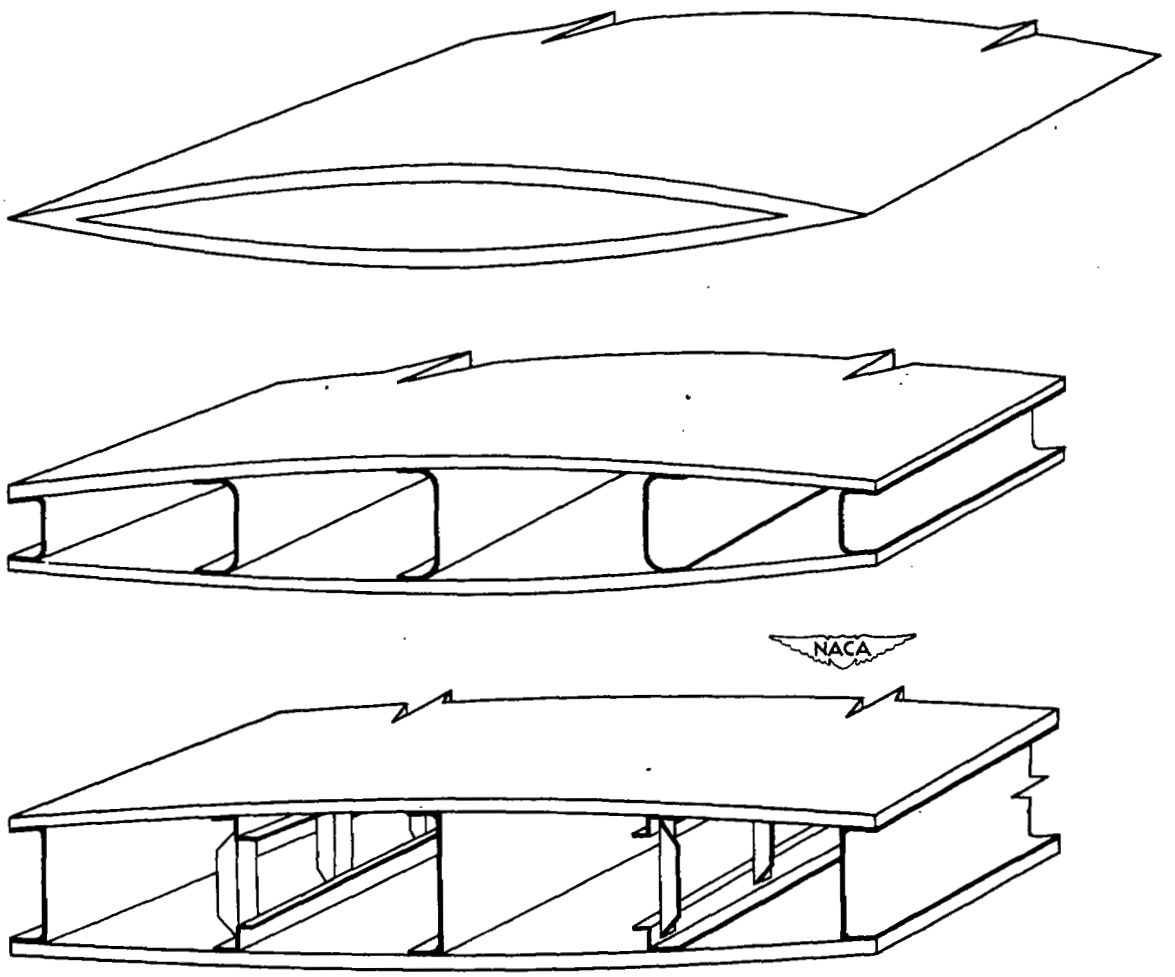

Figure 1.- Types of thick-skin-wing construction.

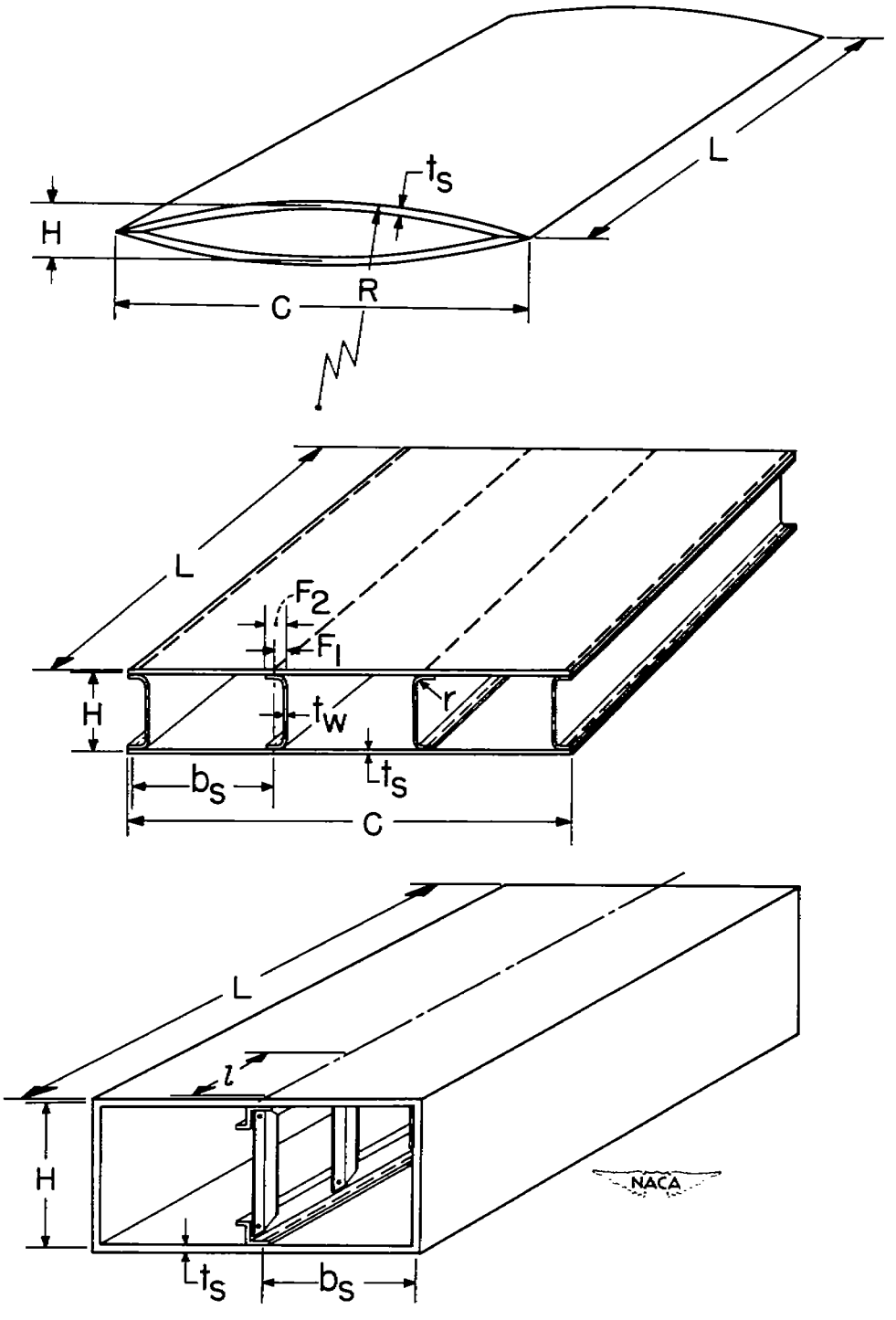

Figure 2.- Types of test specimens. Nominal dimensions listed in tables I, II, and III.

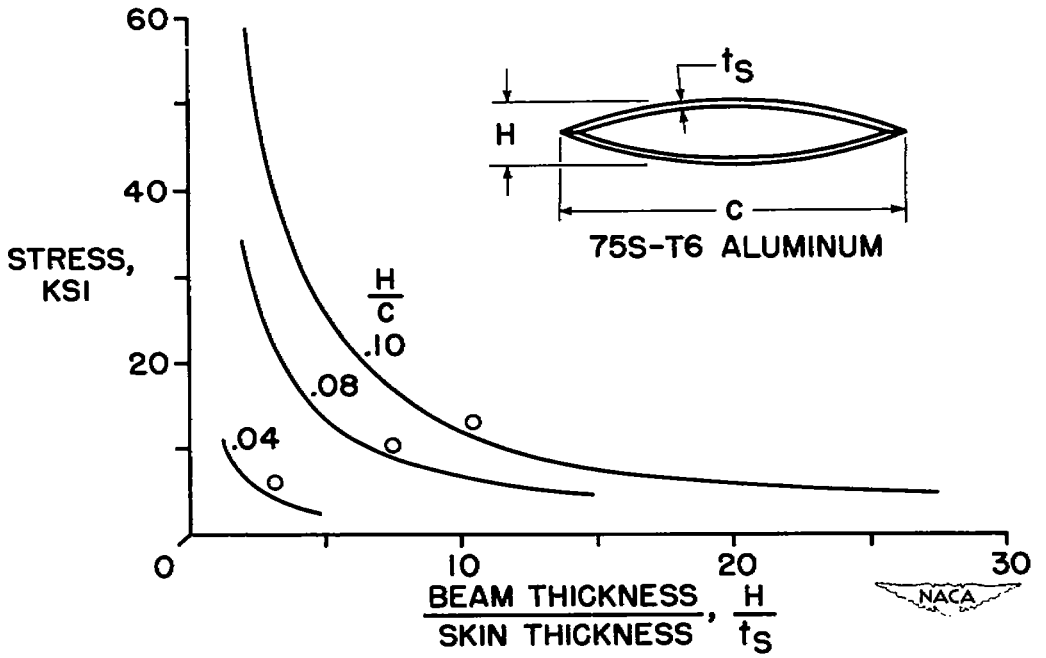

Figure 3.- Bending strength of circular-arc airfoils.

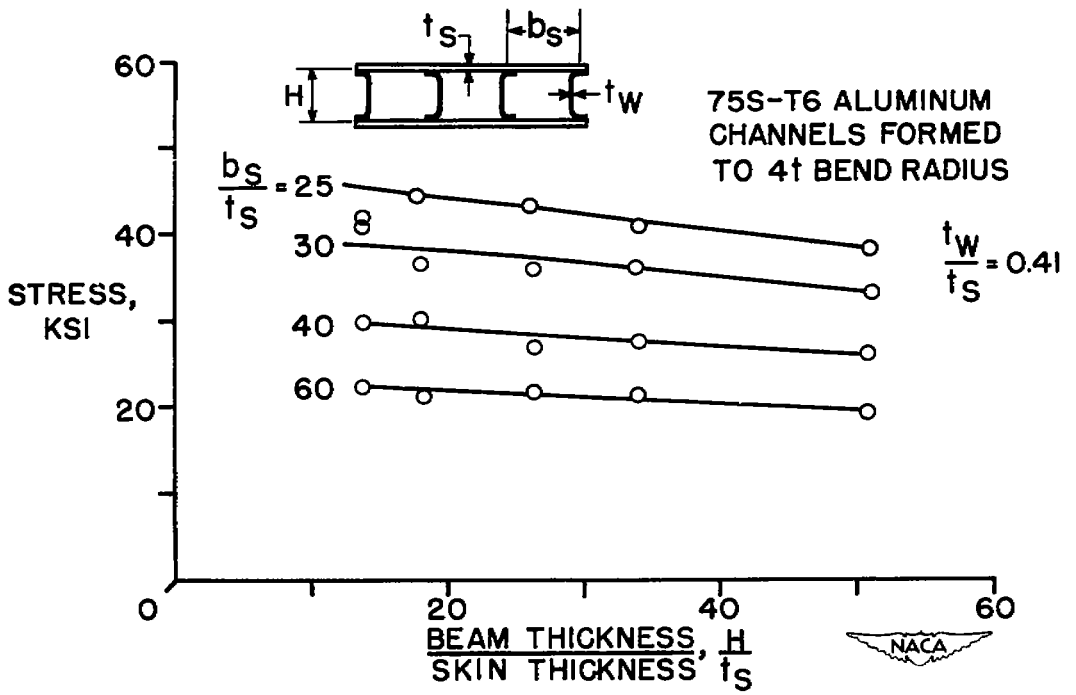

Figure 4.- Bending strength of multiweb beams with formed-channel webs.

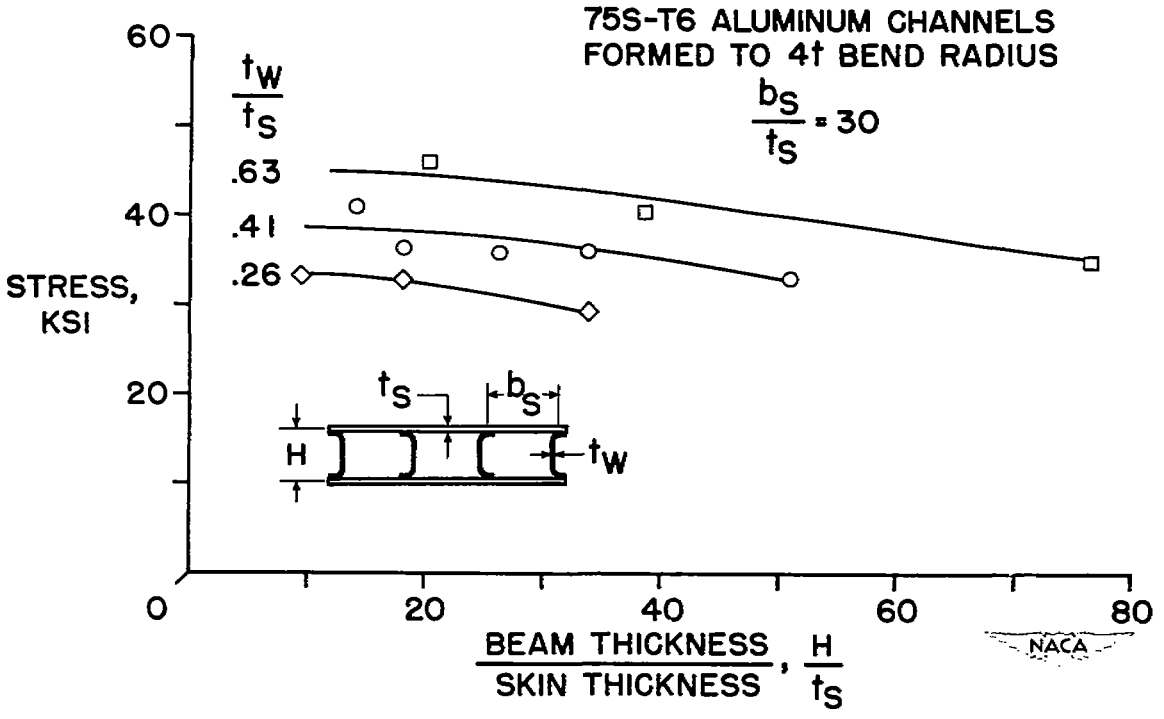

Figure 5.- Effect of web thickness on bending strength of multiweb beams with formed-channel webs.

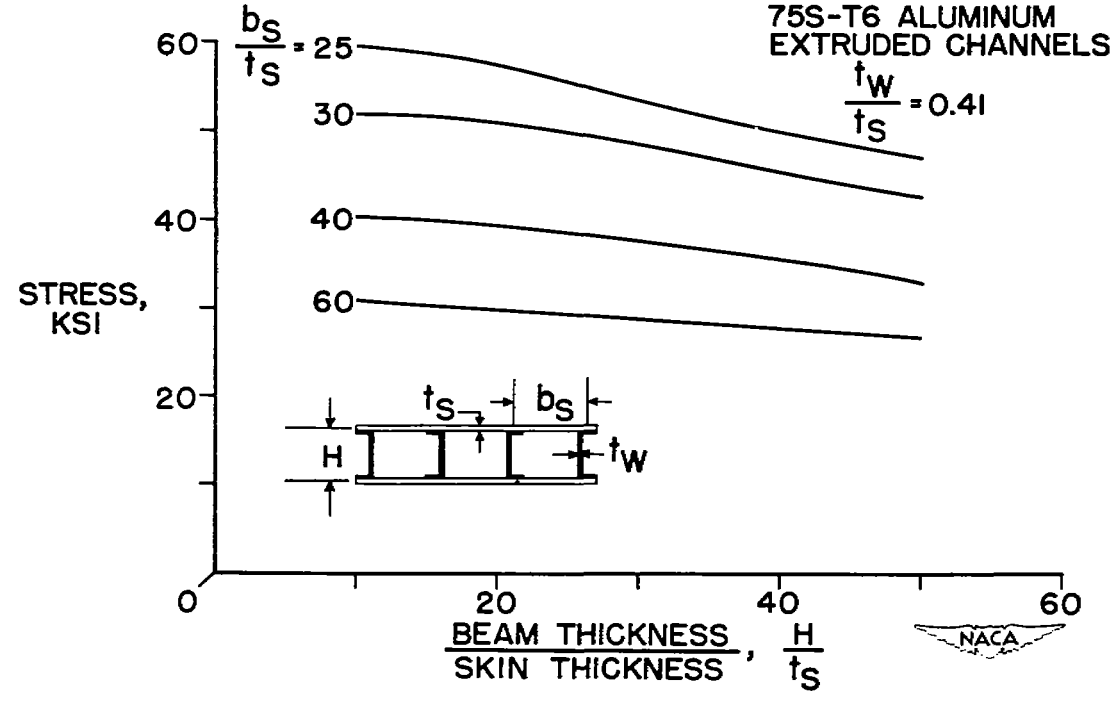

Figure 6.- Predicted bending strength of multiweb beams with extruded channel webs (or web cap members).

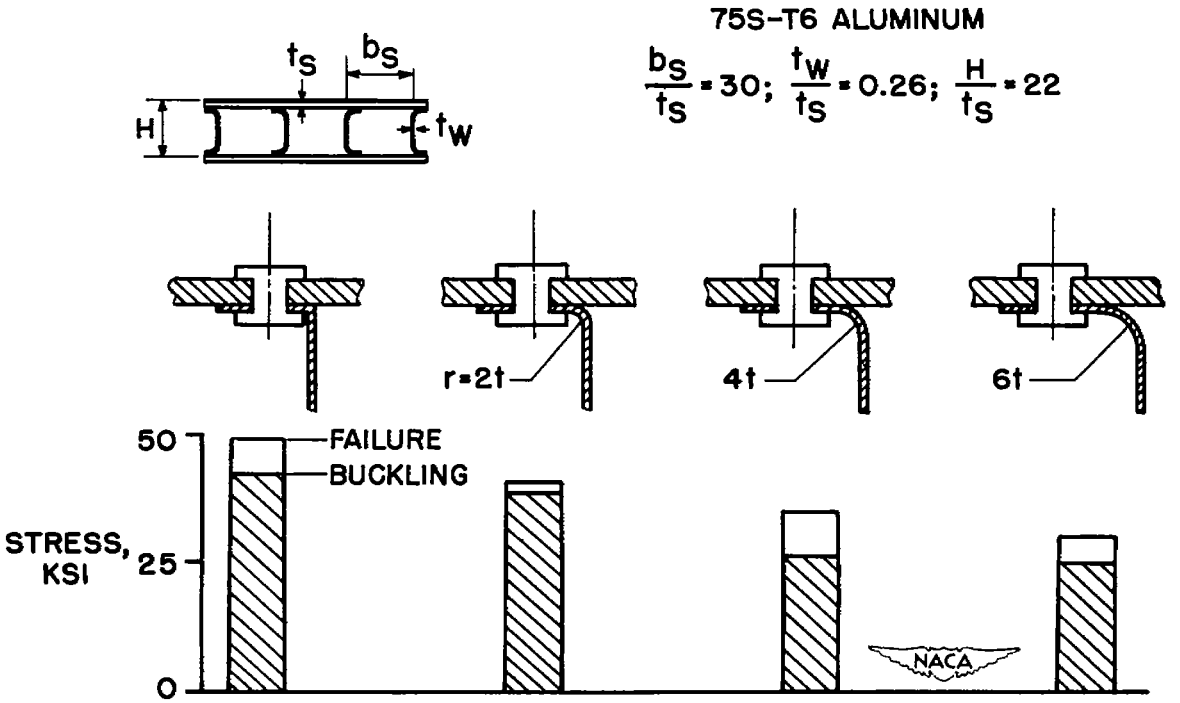

Figure 7.- Effect of web-skin joint design on the bending strength of multiweb beams.

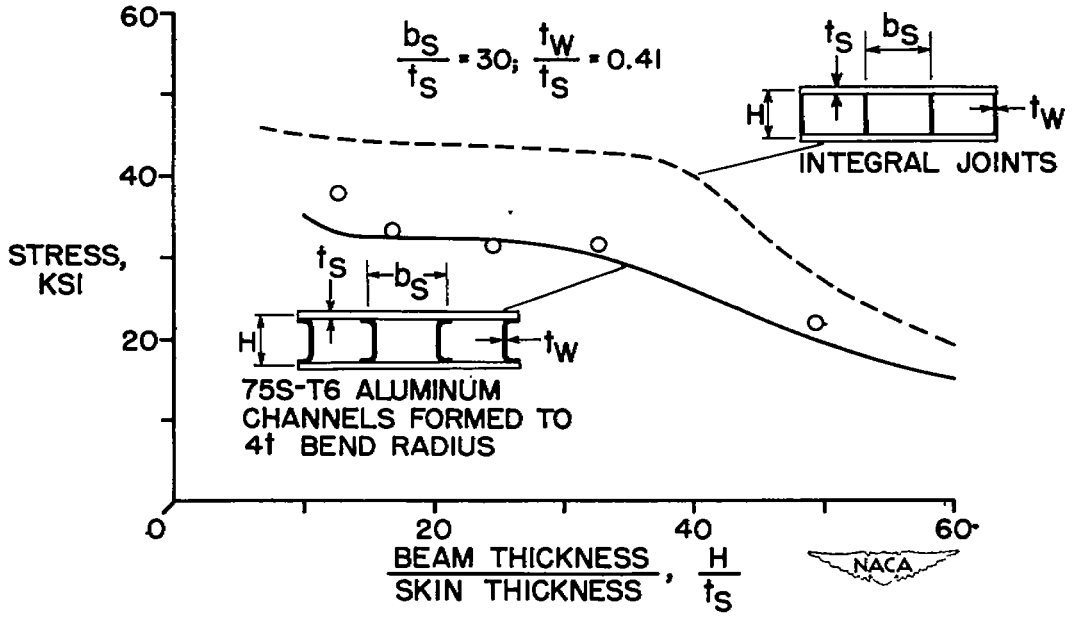

Figure 8.- Comparison of theoretical and experimental buckling stresses for multiweb beams with formed-channel webs.

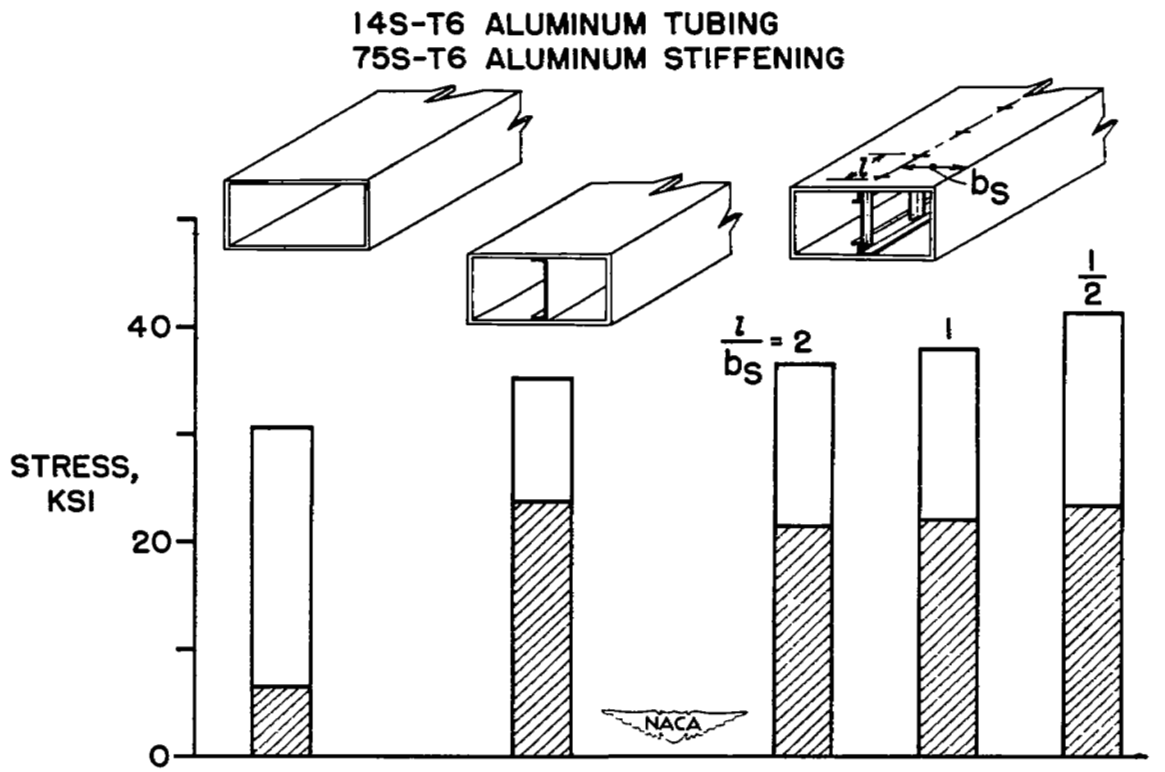

Figure 9.- Comparative bending tests on a beam stiffened by different center line supports.

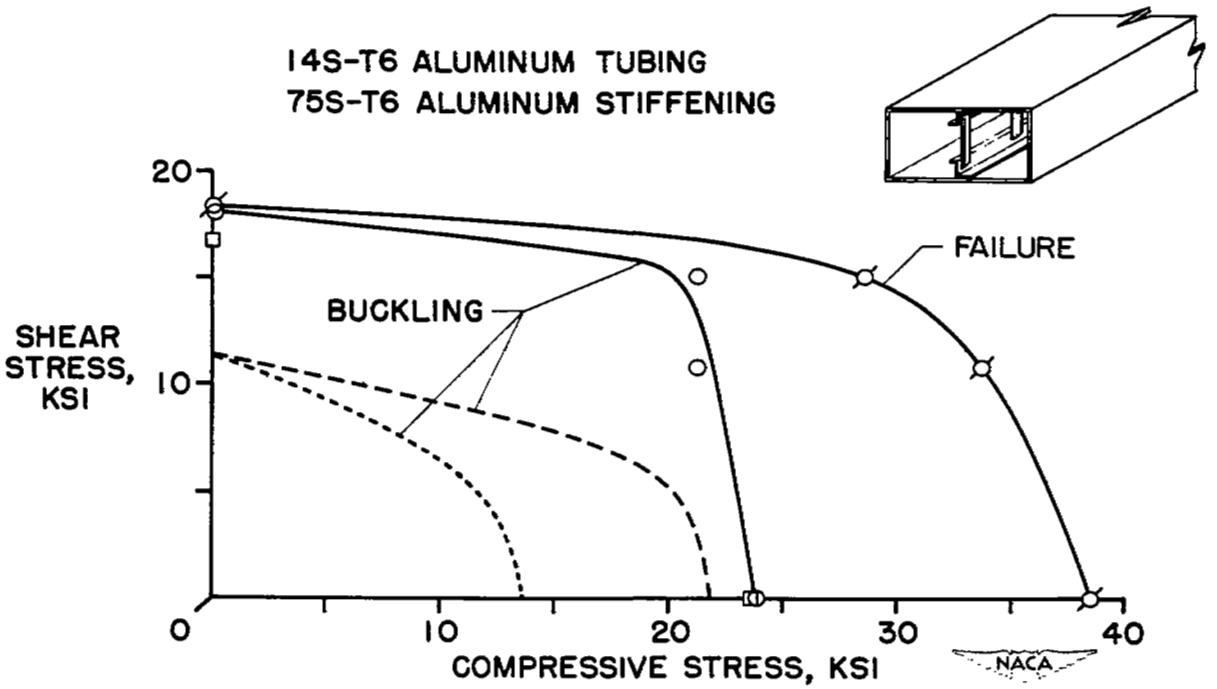

Figure 10.- Interaction of bending and torque on post stiffened beams.

NACA-Langley - 8-27-53 - 325